Analyst

Accepted Manuscript

ROYAL SOCIETY OF CHEMISTRY

www.rsc.org/analyst

Journal Name

RSCPublishing

ARTICLE

Plasma Biomarkers of Pulmonary Hypertension identified by Fourier Transform Infrared Spectroscopy and Principal Component Analysis

Emilia Staniszewska-Slezak[a,b], Andrzej Fedorowicz[b], Karol Kramkowski[c], Agnieszka Leszczynska[c], Stefan Chlopicki[b,d], Malgorzata Baranska[a,b] and Kamilla Malek[a,b*]

Cite this: DOI: 10.1039/x0xx00000x

Received 00th January 2012,
Accepted 00th January 2012

DOI: 10.1039/x0xx00000x

www.rsc.org/

In this work FTIR studies on blood plasma in the rat models of hypertension are reported. The main goal was to find specific spectral markers in plasma of pulmonary arterial hypertension (PAH) induced by monocrotaline injection in rats. FTIR was used to monitor biochemical changes in plasma caused by PAH and to compare them to the systemic hypertension induced by partial ligation on left artery and to the control group. Both pathologies, systemic and pulmonary hypertension, induced a unique response in biochemical content of plasma, mainly related with composition and secondary structure of plasma proteins. For PAH, β-pleated sheet components of plasma proteins were identified whereas protein composition in systemic hypertension is dominated by unordered structures. Additionally, a higher concentration of tyrosine-rich proteins was found in plasma from pulmonary than from systemic hypertension. The differences between both pathologies were identified also in terms of lipid composition/metabolism as well as in the content of RNA and glucose, suggesting that lipid peroxidation appears upon inducing pulmonary hypertension. Generally, this work demonstrates that FTIR spectroscopy supported by principal component analysis (PCA) has a potential to become a fast and non-destructive method for characterization of PAH that consequently could have perspective significance in diagnosis of pulmonary hypertension.

Introduction

FTIR spectroscopy has been widely applied in medical and bioanalytical fields as it has a number of useful advantages to study biological materials such as plasma or serum. This technique is non-destructive, rapid and cost-effective to operate and require simple sample preparation. There are several papers reporting identification of specific biomarkers for various physiological states and diseases in blood components (mainly plasma) using Fourier Transform Infrared spectroscopy.[1-6] For instance, Déléris and Petibois showed that IR spectra of plasma and erythrocytes are sensitive to detect exercise-induced oxidative stress.[1,2] Spectral features observed in FTIR spectra of plasma and erythrocytes indicated changes in bands assigned to fatty acyl moieties, phosphate groups and proteins. The authors suggest that the attack of reactive oxygen species during the oxidative stress primarily affects saturation level of fatty acyl chains and phospholipid structure.[1,2] In turn, Perez-Guaita et. al. employed ATR FTIR technique supported by partial least squares (PLS) method to identify protein profile in serum. This approach included a method of identification and quantification of several serum protein parameters from one ATR FTIR spectrum such as content of total albumin, globulin and immunoglobulin as well as their relative contribution to overall protein composition.[3] Other FTIR studies revealed changes in the content of DNA, RNA and carbohydrates in lymphocytes related to the progression of leukemia.[4,5] Among several applications of vibrational spectroscopy in the analysis of blood components, studies on diabetes showed FTIR technique as a powerful tool in diagnosis of the disease, including the ability to assess the concentration of glucose in plasma/serum/full blood, changes in saturation of fatty acids in platelets, and fluidity of platelets membranes.[6]

In our work we focus on characterisation of pulmonary arterial hypertension (PAH) in plasma by means of transmission FTIR technique. PAH is a chronic progressive disease of the pulmonary vasculature, characterized by elevated pulmonary arterial pressure leading to right ventricular failure.[7,8] In contrast to systemic hypertension that is diagnosed on the basis of a simple systemic blood pressure measurements, the diagnosis of PAH requires a combination of tests, e.g. functional assessment, exercise tolerance, laboratory tests, magnetic resonance imaging, echocardiography to support right heart hypertrophy or failure.[9]

Pulmonary arterial hypertension (PAH) is a rare, progressively worsening disease that still remains incurable. The molecular mechanism of PAH has not been fully understood, but it is characterized by dysfunction of pulmonary endothelium including alterations in bioavailability of NO, synthesis of prostacyclin secretion of endothelin-1 [10,11] and current disease-specific therapeutic interventions in PAH target one of these three established pathways in PAH pathobiology: prostacyclin, nitric oxide, and endothelin-1. There are

numerous other changes in the concentration of plasma mediators associated with PAH including changes in atrial natriuretic peptide, apelin, adrenomedullin, hepcidin[12-14]; thrombomodulin, vascular endothelial growth factor (VEGF), transforming growth factor (TGF-β1), angiopoietin-2,[15-21] and others. However, none of them explicitly indicates pulmonary hypertension. Therefore, searching for an easy blood-based biomarker of PAH is still of interest.

To our best knowledge, FTIR studies on blood components in a model of hypertension have not been reported up to now. Only Saravankumar and co-workers presented FTIR monitoring of biochemical changes caused by systemic hypertension and its treatment in samples of homogenized liver tissue.[22] The main goal of this study was to find a specific fingerprint of PAH induced by monocrotaline injection in rats in plasma by means of FTIR spectroscopy. Additionally, we assessed whether spectral plasma features of PAH differed from these induced by systemic hypertension induced by partial ligation on left artery in rats. In the present work we demonstrated for the first time, that FTIR spectroscopy in combination with principal component analysis (PCA) has the required discrimination ability to become a quick, non-destructive method for characterization of PAH associated changes in plasma that could have potential diagnostic significance in pulmonary hypertension.

Experimental

Animal models

All investigations were performed according to the Guide for Care and Use of Laboratory Animals published by the US National Institutes of Health while the experimental procedure was approved by the local Animal Research Committee, Jagiellonian University.

To induce pulmonary arterial hypertension, male Wistar rats (260-300 g, N=4) were injected with monocrotaline (MCT, 60 mg/kg s.c.; Sigma Aldrich) solution. MCT was dissolved *ex tempore* in 1 M HCl, neutralized with 1 M NaOH and diluted with distilled water. Control group (N=5) was injected with saline. 28 days post-MCT injection, rats were anaesthetized (pentobarbitone, 40 mg/kg, *i.p.*) and blood was collected from right ventricle to the syringe with nadroparine (end-concentration 10U/ml), and then heart was removed. To assess a hallmark of PAH, right ventricular hypertrophy right ventricle was separated from left ventricle and septum. Both parts were weighted and right to left ventricle and septum mass ratio was calculated (RV/(LV+S)W). This ratio increased from 0.325±0,013 for control group to 0.379±0,008 for MCT-treated group ($p<0.05$).

In the model of systemic hypertension, rats were firstly anesthetized with pentobarbital (40 mg/kg, *i.p.*). Two-kidney one-clip (2K1C) renovascular hypertension was induced by a partial, standardised clipping of the left renal artery; N=5. After 6 weeks most of the animals developed hypertension which was confirmed by the blood pressure measurement using the 'tail cuff' method.[23] Rats developing mean blood pressure (MBP) higher than 140 mmHg were considered hypertensive and were used in experiments. Sham-operated rats (SO) served as a control to 2K1C hypertensive rats, N=5. They received the same surgical intervention without the clipping of the renal artery. Blood was collected as described above for the PAH group.

Sample preparation

Blood samples were centrifuged at 1 000*g* for 10 min. and then plasma were immediately separated. Time between blood collection and centrifugation was approx. 10 min. Next, 3 replicates of each plasma sample (0.5 μL) were manually spotted onto CaF_2 windows, and left to dry in a temperature-controlled laboratory (24 °C). The drying process took approximately 5 min giving deposits with ca. 5 mm in diameter. The volume of plasma was adjusted to provide FTIR spectra with absorbance below 1.2. Our previous investigations on FTIR profile of the plasma deposit on the CaF2 window showed its spectral uniformity regarding positions of bands and intensity ratios.[24] In our approach we collect FTIR images close to the periphery of the deposit. We collect three IR images for each plasma deposit. And for each animal, three plasma samples are deposited on a IR window.

FTIR imaging and data processing

Liquid nitrogen cooled MCT FPA (Mercury Cadmium Telluride Focal Plane Array) detector comprising 4096 pixels arranged in a 64×64 grid format was used to measure FTIR images with a Agilent 670-IR spectrometer and 620-IR microscope operating in rapid scan mode. Transmission measurements were performed with a 15× Cassegrain objective collecting 64 scans from a plasma sample deposited on a CaF_2 window. Background measurements were acquired on blank substrates with 128 scans per pixel. All spectra were collected in the range of 3800–900 cm^{-1} with a spectral resolution of 8 cm^{-1} used also in other studies on biological material.[25,26] Recording 4096 spectra took 3 min.

FTIR spectra embedded in each spectral image were first quality-screened and then extracted using a CytoSpec v. 1.4.03 software.[27] The quality test for sample thickness was performed according to the absorbance over the „fingerprint region" (900-1750 cm^{-1}) to remove spectra with the maximum absorbance less than 0.4 or greater than 1.2. Then, ca. 50 spectra for each sample were randomly extracted. As an example, we collect raw FTIR spectra in Figure S1 (in Electronic Supplementary Information) for control and systemic hypertension plasma As seen from this Figure, spectra of plasma are not obscured resonance Mie scattering effect. Additionally, Figure S2 (in ESI) presents FTIR images for the amide I band before and after quality test. The latter show that FTIR spectra of low signal to noise ratio are only removed. Processing of spectral data was performed in OPUS (Version 7.0, Bruker Optic, Ettingen, Germany) and Unscrambler X (version 10.3, Camo Software, Oslo, Norway) software packages.

Using the Opus program, approx. 600 raw spectra for each group were vector normalized in the region of 1800-900 cm^{-1} and then averaged. Second derivatives of mean spectra were calculated by using a Savicky – Golay method (number of smoothing points: 9) to show overall changes in spectral profile of the investigated groups. ~~30 raw spectra for each animal were selected for Principal Component Analysis (PCA) carried out using the Unscrambler software.~~ According to [28,29,30] 30 raw spectra from each plasma groups were analysed by using Principal Component Analysis (PCA) provided by a Unscrambler X (ver. 10.3) software. Data were pre-processed by performing firstly, calculated the second derivative spectra by Savicky – Golay method (number of smoothing points: 9) and then corrected using Extended Multiplicative Signal Correction (EMSC) in the regions of 3100–2800 and 1750–900 cm^{-1}. These steps were made in the order to normalize the spectra accounting for differences in sample thickness, to minimize baseline variation, and provide better visual identification of bands that may have been overlying one another in the raw spectra.[31,32] Second derivative FTIR spectra before and after EMCS correction are shown in Fig. S3 in

ESI. PCA was computed for the "bio-region" (3100–2800 and 1750–900 cm^{-1}) by use of the leave-out-one cross-validation approach and Nipal`s algorithm for PCA decomposition. Seven PCs were chosen for the initial decomposition and 20 iterations were performed for each PC. Two-dimensional (2D) score plots and the corresponding PC loading plots were graphed.

Results and discussion

A comparison of average second derivatives of FTIR spectra for plasma of the controls, pulmonary hypertension and systemic hypertension rats is presented in Figure 1. At first glance, FTIR spectrum of PAH-group (red trace) significantly differs from control group (black trace) in the entire spectral region, whereas spectral changes are not as easily identified in systemic hypertension as compared to healthy animals (green trace almost overlaps with the blue one). FTIR spectra of both control groups are almost overlapped showing good reproducibility in the "bio-region" taking into account differences in animal investigations of both pathologies.

Bands positions are identical in all average spectra and they are collected with the assignment in Table 1. Observed spectral changes mainly include a decrease in intensity of the CH stretching and amide I regions for pulmonary hypertension in comparison to control and systemic hypertension. A pronounced change in FTIR spectrum from the PAH group is also found for a band specific for RNA. In turn, a higher intensity of the C=O stretching vibrations of triglycerides at 1747 cm^{-1} and the CC stretching of tyrosine rich-proteins at 1520 cm^{-1} contributes to spectral characteristics of control group. For clear assessment of spectral variance across the studied group we employed Principal Component Analysis whose score and loading plots reveal subtle changes appearing due to the pathological states.

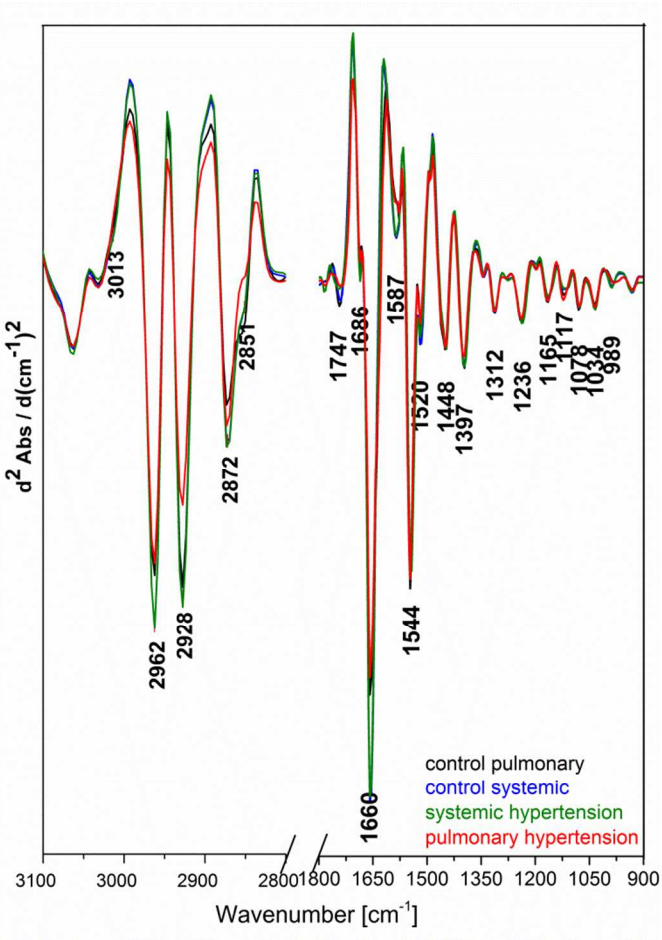

Figure 1. FTIR average second-derivative spectra for plasma of the control groups (black and blue), systemic hypertension (green) and pulmonary hypertension (red) in the 900-1800 and 2800-3100 cm^{-1} (5x enlarged) regions.

Table 1. Position of bands (in cm^{-1}) with their assignment observed in second derivatives FTIR spectra of the plasma studied here.[2,3,6,22,33-39]

Position [cm^{-1}]	Assignment
3013	ν(=CH) unsaturated lipids
2962	$\nu_{as}(CH_3)$ lipids, cholesterol esters, triglycerides, proteins
2928	$\nu_{as}(CH_2)$ lipids, long chain fatty acids, phospholipids
2872	$\nu_s(CH_3)$ proteins, lipids, triglycerides
2851	$\nu_s(CH_2)$ lipids
1747	ν(C=O) lipids, triglycerides, phospholipids, cholesterol esters
1686	ν(C=O) Amide I: antiparallel β-sheets and turns
1656	ν(C=O) Amide I: α-helical structure
1587	$\nu_{as}(COO^-)$ amino acids
1544	δ(N-H) Amide II
1520	ν(CC) tyrosine
1448	$\delta(CH_2, CH_3)$: proteins
1397	$\nu_s(COO^-)$: free fatty acids, free amino acids
1312	Amide III
1236	$\nu_{as}(PO_2^-)$ DNA, phospholipids
1165	ν_{as}(CO-O-C) cholesterol esters
1117	ν(C-O) RNA
1079	$\nu_s(PO_2^-)$ nucleic acids, phospholipids, saccharides
1034	δ(COH) glucose, polysaccharides
989	phosphorylation of proteins, nucleic acids

Pulmonary arterial hypertension *versus* control

Figure 2 shows that the second derivatives of FTIR spectra of plasma from control rats and rats with pulmonary hypertension (PAH) induced by MCT are clustered together in the PC-2 *versus* PC-4 scores plot. PC-4 explains 4% of total variance. The loadings plot shown in Figure 2B indicates that the largest changes in composition of plasma due to inducing PAH are associated with proteins. Along PC-4, the discriminating positively correlated loadings are found for control at 1666 and 1637 cm^{-1} (unordered and β-sheet structures, respectively[36]) whereas negatively correlated loadings are characteristic for PAH and they indicate changes in proteins structures toward α-helices (1650 cm^{-1}) and extended chains and turns (1624 and 1685 cm^{-1}).[33,34] Another feature contributing to segregation of spectra from control plasma and plasma from rats with pulmonary hypertension was a negative loading at 1523 cm^{-1}, originating from tyrosine-rich proteins.[33] Our results show an increase in concentration in Tyr-rich proteins accompanied by changing of secondary structure of proteins toward β-pleated sheet conformation for pulmonary hypertension. Similar FTIR profile was observed for nitration of α-synuclein, suggesting that the approach used here could be useful tool for monitoring this process.[39]

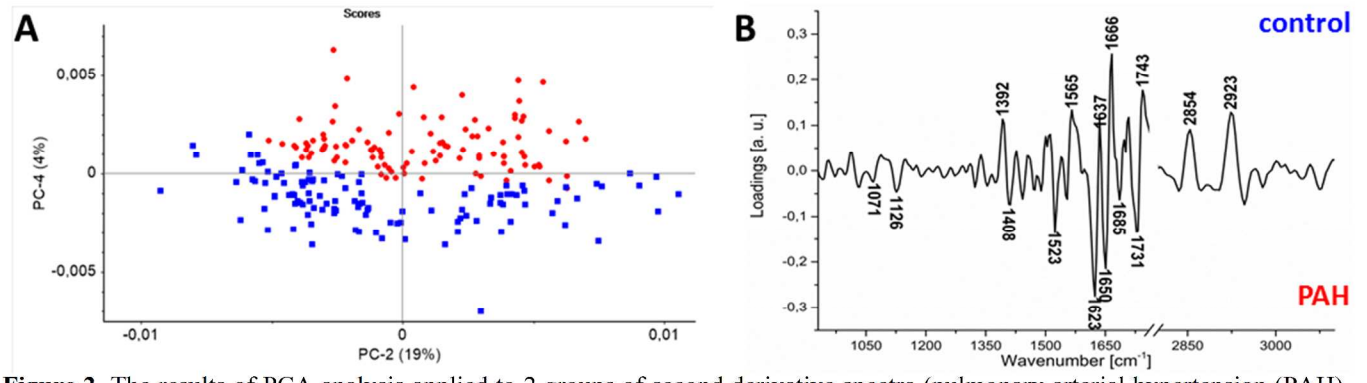

Figure 2. The results of PCA analysis applied to 2 groups of second derivative spectra (pulmonary arterial hypertension (PAH) – red dots from control – blue squares) in the 3100-2800 and 1800-900 cm^{-1} range showing two-dimensional score plot along PC-2 and PC-4 **(A)** and PC-4 correlation loadings plot **(B)**.

The loadings plot also reveals that the discriminating wavenumbers associated with PC-4 appear in the high-wavenumber region and include the asymmetric and symmetric stretching vibrations of the methylene and methyl groups at 2923 and 2854 cm^{-1}. They are positively correlated and thus specific for healthy animals suggesting lipid decomposition due to development of the pathology. This is found in agreement with metabolic changes typical for the disease for that a decrease in concentration of total triglycerides and cholesterol has been observed. Interestingly, the PCA loadings plot also

indicates a shift of the C=O stretching motions from 1743 cm^{-1} in control to 1731 cm^{-1} in pulmonary hypertension. According to the literature[36-38,40] this wavenumber difference corresponds to changes between fractions of triglycerides and esterified cholesterol. However, an increase of concentration of cholesterol esters is not confirmed by the presence of a distinct loading at 1157 cm^{-1}. This may indicate contribution of other esters into these spectral features of plasma of the hypertension model, for example phospholipids.[36] Additionally, the loadings plot shows a strong positive loading at 1392 cm^{-1} shifting to 1408 cm^{-1} for negative correlation. This signal indicates changes in composition of free fatty acids and/or amino acids due to development of pulmonary hypertension.[22,36,37] This can be associated with raising right to left ventricle and septum weight ratio for that the formation of free amino acids is expected.

The PC-4 loading plot also shows that the nucleic acid bands at 1071 [$\nu_s(PO_2^-)$] and 1126 cm^{-1} (RNA) are only discriminators in the spectral region below 1400 cm^{-1}. A higher concentration of nucleic acids is found in plasma of pulmonary hypertension than for control. This can be associated with appearing several types of microRNA in hypertension-related diseases and with the presence of cell-free DNA in plasma.[41-46]

Systemic hypertension *versus* control

Figure 3A illustrates sample grouping for control (blue dots) and systemic hypertension (green squares) induced by partial ligation on left renal artery in the 3100-2800 and 1800-900 cm^{-1} region. ~~Two clusters for both groups are well delineated on the PC-2 *vs.* PC-5 scores plot despite the fact that PC-5 explained 2% of total variance only.~~ Only PC-5 scores plot separates both groups with some overlapping that is found in the agreement with visual inspection of FTIR spectra in Figure 1. PCA scores plots for lower values of the PC did not discriminate both groups, see Fig. S4 (in Electronic Supplementary Material). However, the loadings plot may suggest some biochemical changes in plasma of systemic hypertension. In general, discrimination of both groups is mainly associated with changes in the spectral region of 1740 – 1500 cm^{-1}, see Fig. 3B. Variance is positively correlated with amide I band at 1643 cm^{-1} (characteristic for β-sheet conformation of proteins in control plasma) and negatively correlated with amide I bands at 1666 and 1631 cm^{-1} typical for unordered structure and extended chains in plasma of systemic hypertension.[36] Conformational changes found in the pathology may be associated with phosphorylation process of proteins since the loadings plot shows negative signal at 971 cm^{-1}.[34] It is worthy to mentioned that this protein profile is different than those found for PAH. Our PCA also indicates that clustering is associated with lipids. Positive loadings for control plasma at 2927 and 2854 cm^{-1} (assigned to saturated lipids) and at 1731 and 1157 cm^{-1} (originating from cholesterol esters) suggests decomposition of these macromolecules due to inducing systemic hypertension. This is congruent with appearing a negative signal at 1716 cm^{-1} specific for free fatty acids (in hypertension group).[38-41] In addition, positive and negative loadings at 1411 and 1396 cm^{-1}, respectively, suggest synthesis of fatty acids and/or free amino acids during developing of the disease with different composition than in plasma of the healthy group.[22,36,37]

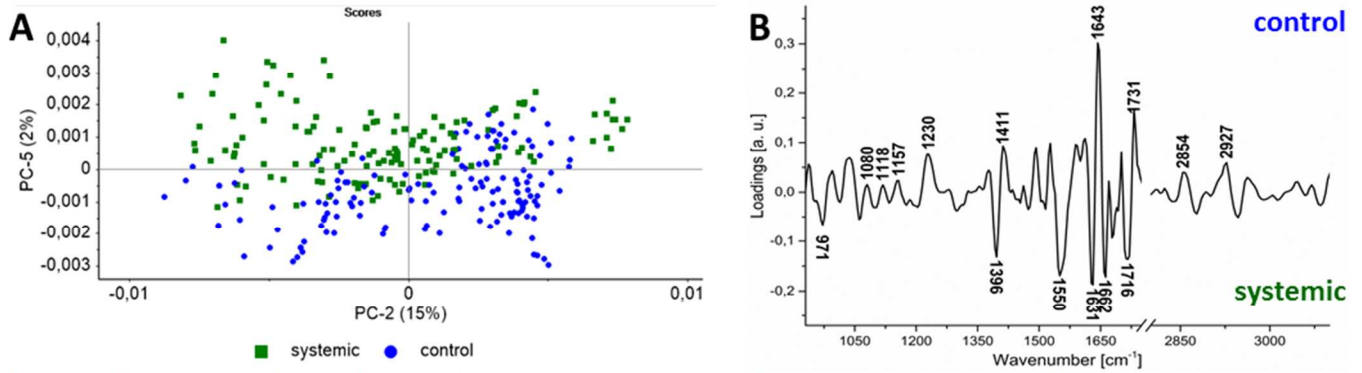

Figure 3. The results of PCA analysis applied to 2 groups of second derivative spectra (systemic hypertension – green squares from control – blue dots) in the 3100-2800 and 1800-900 cm^{-1} range showing two-dimensional score plot along PC-2 and PC-5 (A) and PC-5 correlation loadings plot (B).

Wavenumbers that also contribute to the control – systemic hypertension segregation are found at 1118 [ν(C-O)] and 1230/1080 cm^{-1} [$\nu_{as}(PO_2^-)/\nu_s(PO_2^-)$] in positive loadings of control group. This can indicate that both nucleic acids, DNA and RNA, and/or phospholipids are also involved in biochemical processes reflected in plasma of the systemic hypertension model.[6,35]

Comparison of systemic and arterial pulmonary hypertensions

Two-class discrimination was also used to identify the segregating biochemical entities between systemic and pulmonary hypertensions. Figure 4A shows the score plot for both pathologies; perfect cluster segregation is observed, pointing to PC-1 being most responsible for this observation with 50% of total variance. This clearly indicates that plasma of both hypertensions has a distinctly different biochemical composition. Additionally, we observe in the score plot separation of both hypertension groups into sub-groups due to individual variability between animals. This is commonly observed for biological samples.

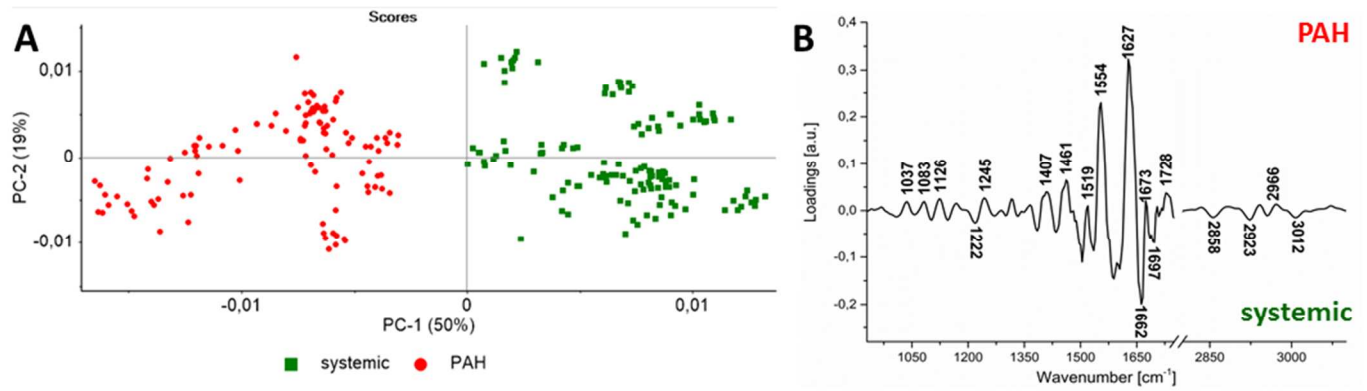

Figure 4. The results of PCA analysis applied to 2 groups of second derivative spectra (systemic hypertension – green dots from pulmonary (PAH) – red squares) in the 3100-2800 and 1800-900 cm^{-1} range showing two-dimensional score plot along PC-1 and PC-2 (A) and PC-1 correlation loadings plot (B).

The major discriminants in the PC-1 loading plot are two positively correlated amide bands at 1627 and 1554 cm^{-1}, characterising β-pleated sheet components of plasma proteins of pulmonary hypertension. While protein composition in systemic hypertension is dominated by unordered structures (negative loading at 1662 cm^{-1}).[34] This separation is consistent with discussed-above discrimination of both hypertension groups from control. Additionally, a higher concentration of tyrosine-rich proteins is found in plasma from pulmonary than from systemic hypertension.

Differences between systemic and pulmonary hypertensions in terms of lipid composition/metabolism are revealed by negative loadings at 3012, 2923 and 2858 cm^{-1}, suggesting that plasma from the pulmonary hypertension model contains a lower concentration of lipids, including unsaturated fraction of these biomolecules. This may also indicate that lipid peroxidation appears upon inducing pulmonary hypertension. The latter is characterised by positive loadings at 1728 and 1407 cm^{-1} corresponding to formation of free fatty acids. A few discriminators are found in the region below 1250 cm^{-1}. The most pronounced feature is a shift of the O-P-O asymmetric stretching band from 1245 cm^{-1} for pulmonary hypertension to 1222 cm^{-1} for systemic hypertension. Such a shift was associated with conformation change for the A-DNA to B-DNA transition.[47] The presence of a positive loading at 1083 cm^{-1} (the symmetric PO_2^- stretching band) for plasma of pulmonary hypertension can additionally support a hypothesis that DNA changes its conformation or is decomposed in the case of systemic hypertension comparing to pulmonary pathology. Plasma for the latter also exhibits a higher content of RNA and glucose (positive loadings at 1126 and 1037 cm^{-1}, respectively).

Conclusions

Here we demonstrate for the first time a potential of FTIR spectroscopy as a method for easy and rapid recognition of pulmonary hypertension by assessment of biochemical changes in plasma that seem to reflect the pathological changes in pulmonary circulation and are not shared by the plasma changes associated with systemic hypertension. The combination of FTIR spectroscopy and multivariate data analysis may prove useful to find novel biomarkers of pulmonary hypertension. The important findings of this work was to show that plasma spectral signature of pulmonary hypertension was significantly different then these for systemic hypertension. These results also indicate that both pathologies systemic and pulmonary hypertension induced a unique response in biochemical contents of plasma that could have diagnostic and prognostic significance. Our PCA analysis implicates that the first targets of further investigations should be plasma fractions to determine the range of peptides/proteins responsible for the observed changes. At this stage of our investigations, it is rather impossible to indicate what plasma proteins are responsible for the found discriminators. As mentioned in the Introduction, the composition of plasma peptides and proteins changes upon the development of the pathology. Additionally, several post-translational modifications of proteins can appear and they result from oxidation, carbonylation, glycation, phosphorylation or conjugation with products of lipid peroxidation. But an exact identification and quantification of modified proteins have been still a challenging task.[48,49] It is also well-known that the process of nitration of tyrosine residue in plasma proteins is associated with cardiovascular pathology.[50] Detailed studies should be also directed towards recognition of nucleic acids profile. On the other hand, while the understanding of the observed spectral changes can give a deeper insight into the mechanism of the pathology, the proposed approach would have many benefits for the prognostic purpose. Introducing the FTIR technique to the clinical environment would greatly enhance the current diagnosis of pulmonary hypertension.

Acknowledgements

This work was supported by National Center of Science (DEC-2013/09/N/NZ4/00597) and by the European Union from the resources of the European Regional Development Fund under the Innovative Economy Programme (grant coordinated by JCET-UJ, No POIG.01.01.02-00-069/09).

Notes

[a]Faculty of Chemistry, Jagiellonian University, Ingardena 3, 30-060 Krakow, Poland.
[b]Jagiellonian Centre for Experimental Therapeutics (JCET), Jagiellonian University, Bobrzynskiego 14, 30-348 Krakow, Poland.
[c]Department of Pharmacodynamics, Medical University in Bialystok, Mickiewicza 2C, 15-222 Bialystok, Poland.
[d]Department of Experimental Pharmacology (Chair of Pharmacology), Jagiellonian University, Grzegorzecka 16, Krakow, 31-531, Poland.

*CORRESPONDING AUTHOR: K. Malek, e-mail: malek@chemia.uj.edu.pl, phone/fax: +48 12 663 2064/+48 12 634 0515

References

1 G. Déléris, C. Petibois, *Vib. Spectrosc.,* 2003, **32**, 129.
2 C. Petibois, G. Déléris, *Cell Biol. Intern.,* 2005, **29**, 709.
3 D. Perez-Guaita, J. Ventura-Gayete, C. Pérez-Rambla, M. Sancho-Andreu, S. Garrigues, M. de la Guardia, *Anal. Bioanal. Chem.,* 2012, **404**, 649.
4 L. Büttner Mostaco- Guidolin, L. Bachmann, *Appl. Spectrosc. Rev.,* 2011, **46**, 388.
5 R. K. Sahu, U. Zelig, M. Huleihel, N. Brosh, M. Talyshinsky, M. Ben-Harosh, S. Mordechai, J. Kapelushnik, *Leukemia Res.,* 2006, **30**, 687.
6 K-Z. Liu, R. Bose, H. H. Mantsch, *Vib. Spectrosc.,* 2002, **28**, 131.
7 R. Patel, W. S. Aronow, L. Patel, K. Gandhi, H. Desai, D. Kaul, S. P. Sahgal, *Med. Sci. Monit.,* 2012, **18**, RA31.
8 Y. Shi, C. Wang, S. Han, B. Pang, N. Zhang, J. Wang, J. Li, *Med. Sci. Monit.,* 2012, **18**, BR69.
9 Y. C. Lai, K. C. Potoka, H. C. Champion, A. L. Mora, M. T. Gladwin, *Circ. Res.,* 2014, **115**, 115.
10 E. Braunwald, D.P. Zipper, P. Libby, *Heart Disease,* 6th edition, W. B. Saunders Company, 2001.
11 R. Budhiraja, R. M. Tuder, P. M. Hassoun, *Circulation*, 2004, **109**, 159.
12 J. Kim, Y. Kang, Y. Kojima, J. K. Lighthouse, X. Hu, M. A. Aldred, D. L. McLean, H. Park, S. A. Comhair, D. M. Greif, S. C. Erzurum, H. J. Chun, *Nat. Med.*, 2013, **19**, 74.
13 S. Murakami, H. Kimura, K. Kangawa, N. Nagaya, *Cardiovasc. Hematol. Disord. Drug Targets,* 2006, **6**, 125.
14 C. D. Vizza, C. Letizia, L. Petramala, R. Badagliacca, R. Poscia, E. Zepponi, E. Crescenzi, A. Nona, G. Benedetti, F. Farrante, S. Sciomer, F. Fedele, *Regul Peptides*, 2008, **151**, 48.
15 N. Selimovic, C. H. Bergh, B. Andersson, E. Sakiniene, H. Carlsten, B. Rundqvist, *Eur. Respir. J.*, 2009, **34**, 662.
16 M. Duncan, B. D. Wagner, K. Murray, J. Allen, K. Colvin, F. J. Accurso, D. D. Ivy, *Mediat. Inflamm.,* 2012, **2012**, 143428.
17 A. A. Lopes, L. H. Caramurú, N. Y. Maeda, *Clin. Appl. Thromb-Hem.,* 2002, **8**, 353.
18 L. Maricić, A. Vceva, R. Visević, A. Vcev, M. Milić, V. Serić, V. Fijacko, *Coll. Antropol.,* 2013, **37**, 1153.
19 G. Cella, F. Vianello, F. Cozzi, H. Marrota, F. Tona, G. Saggiorato, O. Iqbal, J. Fareed, *J. Rheumatol.*, 2009, **36**, 760.
20 A. Filusch, E. Giannitsis, H. A. Katus, F. J. Meyer, *Clin. Sci. (Lond).*, 2010, **119**, 207.
21 L. Tul, F. S. De Man, B. Girerd, A. Huertas, M. C. Chaumais, F. Lecerf, C. François, F. Perros, P. Dorfmüller, E. Fadel, D. Montani, S. Eddahibi, M. Humbert, C. Guignabert, *Am. J. Respir. Crit. Care Med.,* 2012, **186**, 666.
22 M. Saravankumar, J. Manivannan, J. Sivasubramanin, T. Silambrasan, E. Balamurugan, B. Raja, *Mol. Cell Biochem.*, 2012, **362**, 203.
23 R. Zatz, *Lab Anim. Sci*., 1990, **40**, 198.
24 E. Staniszewska-Slezak, A. Rygula, K. Malek, M. Baranska, "Transmission versus transflection mode in FTIR analysis of blood plasma: is the EFSW effect the only reason of the observed spectral distortions?", Analyst (2014) submitted.
25 C. Chonanant, K. R.Bambery, N. Jearanaikoon, S. Chio-Srichan, T. Limpaiboon, M. J. Tobin, P. Heraud, P. Jearanaikoon, *Talanta*, 2014, **130**, 39.
26 J. Cao, E. S. Ng, D. McNaughton, E. G. Stanley, A. G. Elefanty, M. J. Tobin, P. Heraud, *J. Biophotonics,* 2014, **7**, 767.
27 www.cytospec.com
28 A. Khoshmanesh, M. W. A. Dixon, S. Kenny, L. Tilley, D. McNaughton, B. R. Wood, *Anal. Chem.*, 2014, **86**, 4379.
29 E. Lipiec, K. R. Bambery, P. Heraud, W. M. Kwiatek, D. McNaughton, M. J. Tobin, C. Vogel, B. R. Wood, *Analyst*, 2014, **139**, 4200.
30 J. Ollesch, S. L. Drees, H. M. Heise, T. Behrens, T. Brüning, K. Gerwert, *Analyst*, 2013, **138,** 4092.
31 K. Thumanu, S. Sangrajrang, T. Khuhaprema, A. Kalalak, W. Tanthanuch, S. Pongpiachan, P. Heraud, *J. Biophotonic*, 2014, **7**, 222.
32 D. Te, W. Tanthanuch, K. Thumanu, A. Sangmalee, R. Parnpai, P. Heraud, *Analyst*, 2012, **137**, 4774.
33 M. Harz, C. L. Bockmayer, P. Rösch, R. A. Claus, J. Popp, *Med. Laser Appl.*, 2007, **22**, 87.
34 V. G. Gregoriou, V. Jayaraman, X. Hu, T. G. Spiro, *Biochemistry*, 1995, **34**, 6876.
35 E. Peuchant, S. Richard-Harston, I. Bourdel-Marchasson, J.-F. Dartigues, L. Letenneur, P. Barberger-Gateau, S. Arnaud-Dabernat, J.-Y. Daniel, *Transl. Res.*, 2008, **152**, 103.
36 C. Petibois, G. Cazorla, J.-R. Poortmans, G. Déléris, *Sports Med.,* 2003, **33**, 83.
37 C. Krafft, R. Salzer, G. Soff, M. Meyer-Hermann, *Cytom. Part A*, 2005, **64A**, 53.
38 K. Sato, M. Seimiy, Y. Kodera, A. Kitamura, F. Nomura, *Clin. Chim. Acta*, 2010, **411**, 285.
39 V. N. Uversly, G. Yamin, L. A. Munishkina, M. A. Karymov, I. S. Millett, S. Doniach, Y. L. Lyubchenko, A. L. Fink, *Mol. Brain Res*., 2005, **134**, 84.
40 T. P. Wrobel, L. Mateuszuk, S. Chlopicki, K. Malek, M. Baranska, *Analyst*, 2011, **136**, 5247.
41 S. Pullamsetti, L. Kiss, H. A. Ghofrani, R. Voswinckel, P. Haredza, W. Klepetko, C. Aigner, L. Fink, J. P. Muyal, N. Weissmann, F. Grimminger, W. Seeger, R.T. Schermuly, *FASEB J*., 2005, **19**, 1175.
42 G. Warwick, E. Kotlyar, S. Chow, P. S. Thomas, D. H. Yates, *J. Breath Res.*, 2012, **6**, 036006.
43 C. J. Rhodes, J. Wharton, R. A. Boon, T. Roexe, H. Tsang, B. Wojciak-Stothard, A. Chakrabarti, L. S. Howard, J. S. R. Gibbs, A. Lawrie, R. Condliffe, C. A. Elliot, D. G. Kiely, L. Huson, H. A. Ghofrani, H. Tiede, R. Schermuly, A. M. Zeiher, S. Dimmeler, M. R. Wilkins, *Am. J. Respir. Crit. Care Med.,* 2013, **187**, 294.
44 K. Schlosser, R. J. White, D. J. Stewart, *Am. J. Respir. Crit. Care Med.*, 2013, **188**, 1472.
45 C. Wei, H. Henderson, C. Spradley, L. Li, I. K. Kim, S. Kumar, N. Hong, A. C. Arroliga, S. Gupta, *PLoS One*, 2013, **23**, e64396.
46 C. J. Rhodes, J. Wharton, L. Howard, J. S. Gibbs, A. Vonk-Noordegraaf, M. R. Wilkins, *Eur. Respir. J.,* 2011, **38**, 1453.

47 D. R. Whelan, K. R. Bambery, P. Herauld, M. Tobin, M. Diem, D. McNaughton, B. R. Wood, *Nucleic Acids Res*., 2011, **39**, 5439.
48 M. A. Baraibar, R. Ladouce, B. Friguet, *J. Proteomics*, 2013, **92**, 63.
49 C. M. Spickett, A. Reis, A. R. Pitt, *Anal. Chem*., 2013, **85**, 4621.
50 G. Peluffo, R. Radi, *Cardiovasc. Res*., 2007, **75**, 291.